Supporting Information

Rare-earth hydroxide/MXene hybrid: a promising agent for near-infrared photothermy and magnetic resonance imaging

Mingjun Bai,[a,b,c] Linawati Sutrisno,[d,e] Junhong Duan,[f] Hao Wan,[*b] Gen Chen,[g] Xiaohe Liu,[*b,g] and Renzhi Ma[*c]

[a] College of Materials Science and Engineering, Chongqing University of Technology, Chongqing 400054, P. R. China
[b] Zhongyuan Critical Metals Laboratory, Zhengzhou University, Zhengzhou 450001, P. R. China. E-mail: wanhao@zzu.edu.cn, liuxh@csu.edu.cn
[c] Research Center for Materials Nanoarchitectonics (MANA), National Institute for Materials Science (NIMS), Tsukuba, Ibaraki 305-0044, Japan. E-mail: MA.Renzhi@nims.go.jp
[d] Department of Materials Science and Engineering, Graduate School of Pure and Applied Sciences, Tsukuba, Ibaraki 305-8577, Japan
[e] Research Center for Functional Materials, National Institute for Materials Science (NIMS), Tsukuba, Ibaraki 305-0044, Japan
[f] Department of Radiology, The Third Xiangya Hospital, Central South University, Changsha, Hunan 410013, P. R. China
[g] School of Materials Science and Engineering, Central South University, Changsha, Hunan 410083, P. R. China

Experimental section

Synthesis of nanosheets

The layered gadolinium hydroxide (LGdH) nanosheet was synthesized according to our previous report.[1] That is, the parent LGdH crystals were synthesized via the micro-assistant homogeneous precipitation method, the obtained precipitation was washed and dried in air condition, followed by sonication exfoliation in formamide and centrifuge to remove the unexfoliated particles.

The Ti_3C_2 MXene nanosheet was synthesized by selective etching of the bulk Ti_3AlC_2 powder.[2, 3] Bulk Ti_3AlC_2 was purchased from 11 Technology Co., Ltd. 1.0 g of lithium fluoride (LiF) powder was fully dissolved in 20 mL of 9 M hydrochloric acid (HCl), and then, 0.5 g of Ti_3AlC_2 powder was slowly added into the solution with continues stirring for 24 h at 35 °C for etching. The etched product was washed with deionized water several times until the pH of the solution was ~6. The Ti_3C_2 nanosheet was obtained by sonication of the suspension for 1 h with the protection of nitrogen gas, followed by centrifuging at 3500 rpm for 15 min.

Synthesis of GTC hybrid

GTC hybrids were synthesized by dropwise adding Ti_3C_2 nanosheet suspension into LGdH nanosheet suspension at a designated surface area ratio of 1: 1 under continuous stirring, followed by washing and redispersion in deionized water with the protection of nitrogen gas. The mass ratio was calculated in **Fig. S5** to obtain a theoretic surface area ratio of 1: 1. The LGdH and Ti_3C_2 MXene nanosheets were directly restacked to form flocculates, as LGdH nanosheet is positively charged while Ti_3C_2 nanosheet is negatively charged.

Materials Characterization

Scanning electron microscopy (SEM) was conducted at a JEOL JSM-6700FT microscope. Powder X-ray diffraction (XRD) patterns were collected on a Rigaku Ultima IV diffractometer with Cu Ka radiation (λ=0.15406 nm). Chemical compositions were analyzed by inductively coupled plasma-optical emission spectrometry (ICP-OES) with a Shimadzu ICPS8100CL. The atomic force microscopy (AFM) observations were carried out using a Hitachi AFM5200S in tapping mode. Optical absorption spectra were recorded using a quartz cuvette (light path length: 1 cm) on a UV-vis spectrophotometer (Hitachi, U-4100). Transmission electron microscope (TEM) was performed on

a Tecnai G2 F20. The average hydrodynamic size was quantified by dynamic light scattering (DLS) using a Zetasizer Nano ZS analyzer. Zeta potential was measured using a Zetasizer Nano ZS analyzer. The photothermal performance was investigated using a Thorlabs Inc. NIR laser irradiation at intensities of 2 W cm^{-2}. The temperature change was monitored using an IR thermal camera while the temperature was measured with an electronic thermometer (As one Corp). Magnetic resonance imaging (MRI) scanning was performed by using a Philips Ingenia Elition 3.0 T X MR equipment. Both *in vitro* and *in vivo* T1 images were acquired by using a coronal and transverse magnetization prepared rapid spin echo sequence, the repetition and echo time was 500 ms and 20 ms, respectively. The as-prepared GTC were dispersed in normal saline at various concentrations of 0, 0.15, 0.3, 0.6, 1.25, and 2.5 mg mL^{-1} and were load separately into 2 mL tubes for the testing. For the animal study, the C57 mice were purchased from the Experimental Animal Center of the Third Xiangya Hospital (SYXK2020-0019, Changsha, China) and all animals in this study were in accordance with the guidelines of the Institutional Animal Care and Use Committee. GTC saline suspension (0.125 mg L^{-1}) was subcutaneously injected into one thigh of the nude mouse, 30 minutes later, the T1-weighted *in vivo* MRI measurement was conducted on the mice.

Table S1. Concentrations of different samples in Fig. 3.

Sample number	Ti_3C_2 suspensions (g mL^{-1})	GTC suspensions (g mL^{-1})
S1	0.1800	0.1560
S2	0.0900	0.0780
S3	0.0360	0.0390
S4	0.0270	0.0156
S5	0.0180	0.0078
S6	0.0090	/

Table S2. Comparison of mass extinction coefficient of different photothermal materials.

Materials	Mass extinction coefficient (L g^{-1} cm^{-1})	Wavelength (nm)
GTC (This work)	50.0	808
Ti_3C_2 nanosheet[4]	29.1	808
Ti_3C_2 nanosheet[5]	28.6	808
GdW_{10}@Ti_3C_2[6]	22.4	808
Au nanorods[7]	13.9	808
Carbon nanotubes[8]	46.5	808
Nano-rGO[9]	24.6	808
GO[10]	16.6	808
BCP-MoS_2[11]	14.5	808
BP nanostrucure[12]	20.6	808
Mo_4VC_4[13]	34.4	550
1T-MoS_2[14]	25.6	1064

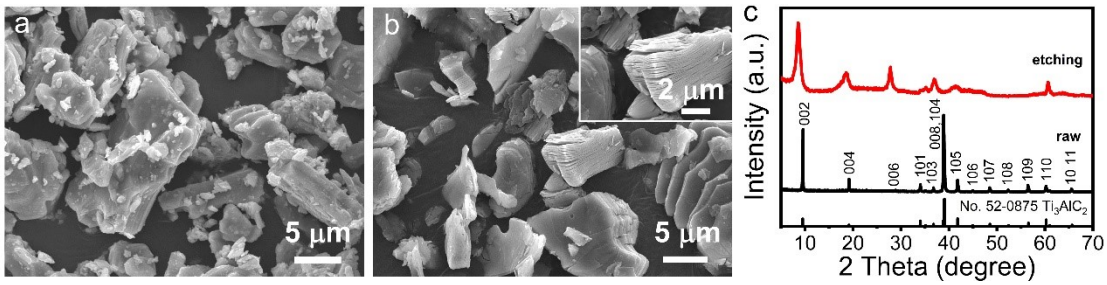

Fig. S1 SEM images of Ti_3AlC_2 particles (a) before and (b) after etching. (c) XRD patterns of Ti_3AlC_2 particles before and after etching. Inset in (b) is an enlarged view showing visible expansion.

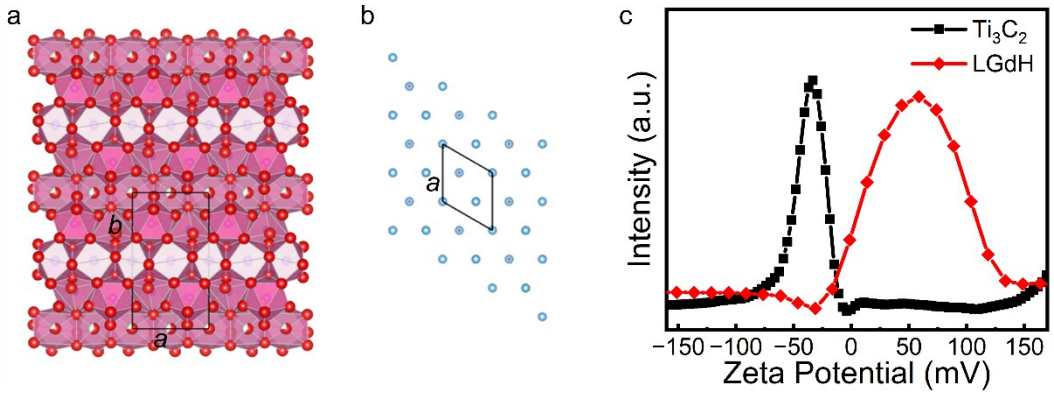

Fig. S2. A hypothesized area-matching model of LGdH and Ti_3C_2 nanosheets based on face-to-face stacking. (a) In-plane structure of LGdH with a rectangular unit cell: a = 1.29 nm, b = 0.73 nm. The 2D mass density $A_1 = M(LGdH)/[a \times b \times N_A] = 0.282 \times 10^{-2}$ g m^{-2}, where $M(LGdH)$ and N_A is the molecular mass of LGdH nanosheet and the Avogadro constant, respectively. (b) In-plane structure of Ti_3C_2 with a rhombus unit cell: a = 0.38 nm. The 2D mass density $A_2 = M(Ti_3C_2)/[a \times b \times \mathrm{Sin}120^\circ \times N_A] = 0.335 \times 10^{-2}$ g m^{-2}, where $M(Ti_3C_2)$ is the molecular mass of Ti_3C_2 nanosheet. The ideal LGdH and Ti_3C_2 structure is used for the estimation. Therefore, the final mass ratio (W) for LGdH and Ti_3C_2 nanosheet under the theoretic surface area of 1: 1 is $W(LGdH)/\ W(Ti_3C_2) = A_1/A_2 = 0.84: 1$. (c) Zeta potential of suspensions containing Ti_3C_2 and LGdH nanosheets, separately.

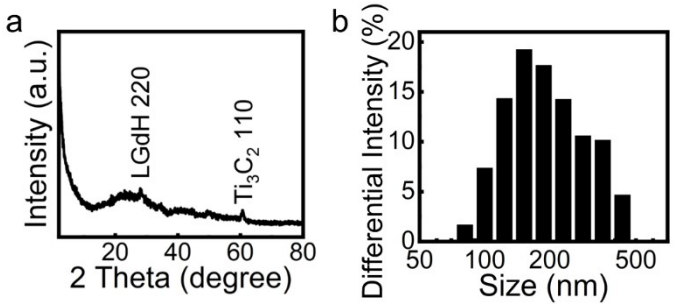

Fig. S3. (a) XRD pattern and (b) DLS size distribution histogram of GTC hybrid.

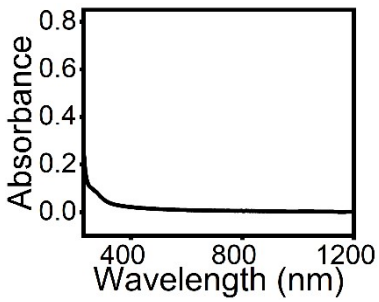

Fig. S4. UV-vis absorption of LGdH nanosheet suspension.

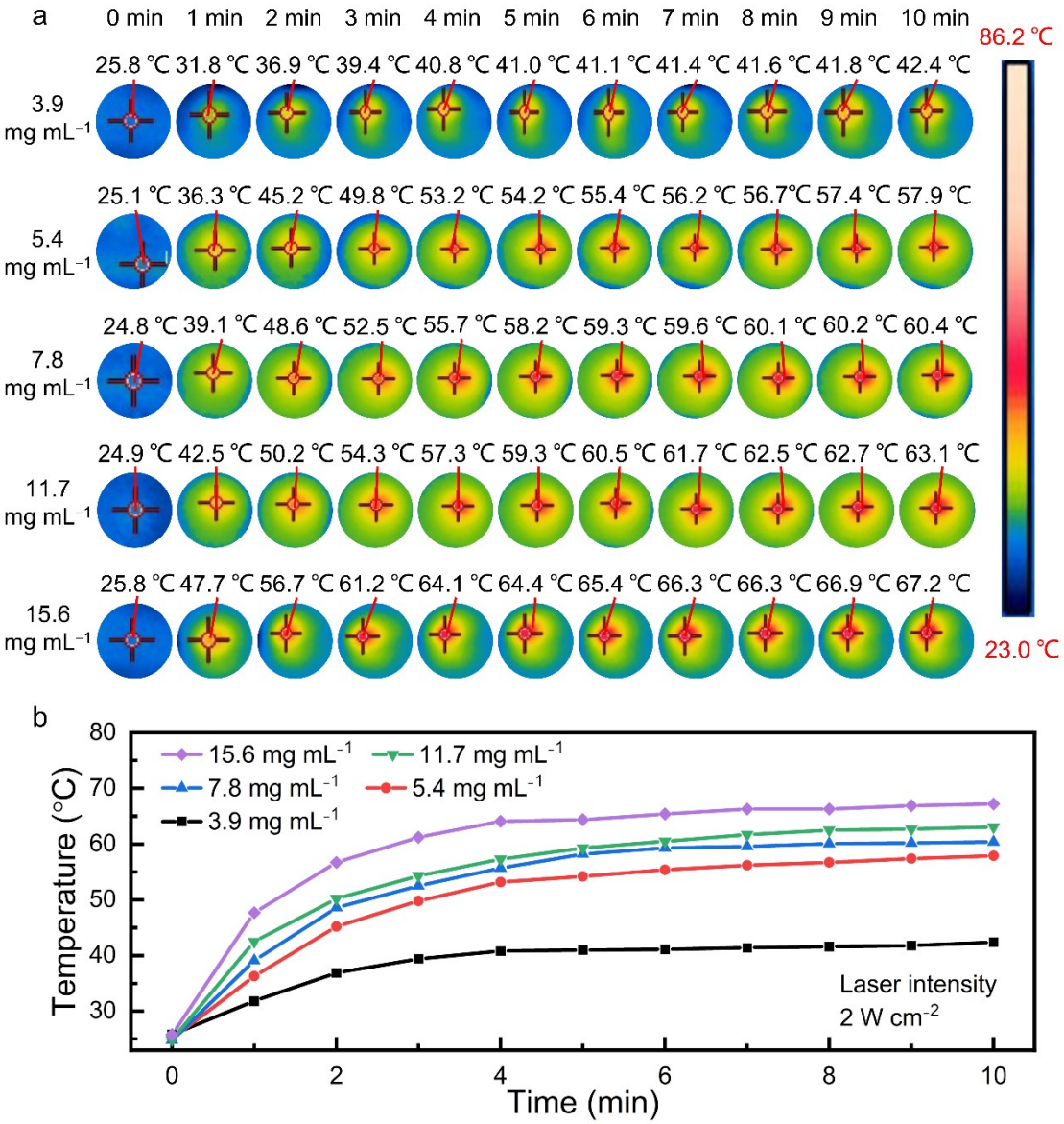

Fig. S5. Photothermal effect of the GTC hybrids. (a) IR thermographic images and (b) heating curves of GTC at different concentrations under NIR laser irradiation (808 nm, 2 W cm^{-2}).

References

1. M. Bai, X. Liu, T. Sasaki and R. Ma, *Nanoscale*, 2021, **13**, 4551-4561.
2. S. J. Kim, J. Choi, K. Maleski, K. Hantanasirisakul, H.-T. Jung, Y. Gogotsi and C. W. Ahn, *ACS Appl. Mater. Interfaces*, 2019, **11**, 32320-32327.
3. J. Ma, Y. Cheng, L. Wang, X. Dai and F. Yu, *Chem. Eng. J.*, 2020, **384**, 123329.
4. J. Xuan, Z. Wang, Y. Chen, D. Liang, L. Cheng, X. Yang, Z. Liu, R. Ma, T. Sasaki and F. Geng, *Angew. Chem. Int. Ed. Engl.*, 2016, **55**, 14569-14574.
5. G. Liu, J. Zou, Q. Tang, X. Yang, Y. Zhang, Q. Zhang, W. Huang, P. Chen, J. Shao and X. Dong, *ACS Appl. Mater. Interfaces*, 2017, **9**, 40077-40086.
6. L. Zong, H. Wu, H. Lin and Y. Chen, *Nano Res.*, 2018, **11**, 4149-4168.
7. J. T. Robinson, K. Welsher, S. M. Tabakman, S. P. Sherlock, H. Wang, R. Luong and H. Dai, *Nano Res.*, 2010, **3**, 779-793.
8. Z. Liu, C. Davis, W. Cai, L. He, X. Chen and H. Dai, *Proc. Natl. Acad. Sci. USA*, 2008, **105**, 1410-1415.

9. J. T. Robinson, S. M. Tabakman, Y. Liang, H. Wang, H. Sanchez Casalongue, D. Vinh and H. Dai, *J. Am. Chem. Soc.*, 2011, **133**, 6825-6831.
10. M. Hashemi, M. Omidi, B. Muralidharan, H. Smyth, M. A. Mohagheghi, J. Mohammadi and T. E. Milner, *ACS Appl. Mater. Interfaces*, 2017, **9**, 32607-32620.
11. C. H. Park, H. Yun, H. Yang, J. Lee and B. J. Kim, *Adv. Func. Mater.*, 2017, **27**, 1604403.
12. M. Qiu, D. Wang, W. Liang, L. Liu, Y. Zhang, X. Chen, D. K. Sang, C. Xing, Z. Li, B. Dong, F. Xing, D. Fan, S. Bao, H. Zhang and Y. Cao, *Proc. Natl. Acad. Sci. USA*, 2018, **115**, 501.
13. G. Deysher, C. E. Shuck, K. Hantanasirisakul, N. C. Frey, A. C. Foucher, K. Maleski, A. Sarycheva, V. B. Shenoy, E. A. Stach, B. Anasori and Y. Gogotsi, *ACS Nano*, 2020, **14**, 204-217.
14. Z. Zhou, B. Li, C. Shen, D. Wu, H. Fan, J. Zhao, H. Li, Z. Zeng, Z. Luo and L. Ma, *Small*, 2020, **16**, 2004173.